Clean Technologies and Environmental Policy
https://doi.org/10.1007/s10098-024-02811-4

ORIGINAL PAPER

Simultaneous biosorption of acid violet and reactive yellow dyes by *Cladosporium cladosporioides*

Can Serkan Keskin[1] · **Semra Yılmazer Keskin**[1] · **Mehmet Can Topcu**[2]

Received: 29 November 2023 / Accepted: 7 March 2024

Abstract

The synthetic dye mixture of Acid Violet 90 and Reactive Yellow 145 was treated with dead *Cladosporium cladosporioides* biomass. The individual concentrations were calculated with the first-order derivative spectrophotometric method. The calibration curves were plotted at wavelengths of 578.4 nm and 318.2 nm in the derivative spectrum for Acid Violet 90 and Reactive Yellow 145, respectively. The calculated limit of quantitation value is ~ 2.5 mg/L for Acid Violet 90 and ~ 1.5 mg/L for Reactive Yellow 145. The achieved mean recovery percentage values are around 100%. The highest removal efficiency (100%) was obtained for both dyes at pH 4 using 0.25 g biomass and 50 mg/L of each dye in 60 min reaction time with 150 rpm shaking speed. The hydrochloric acid solution was used for biomass regeneration, and the removal efficiencies remained at 99% and 89% for Acid Violet 90 and Reactive Yellow 145 in the third cycle.

Graphical abstract

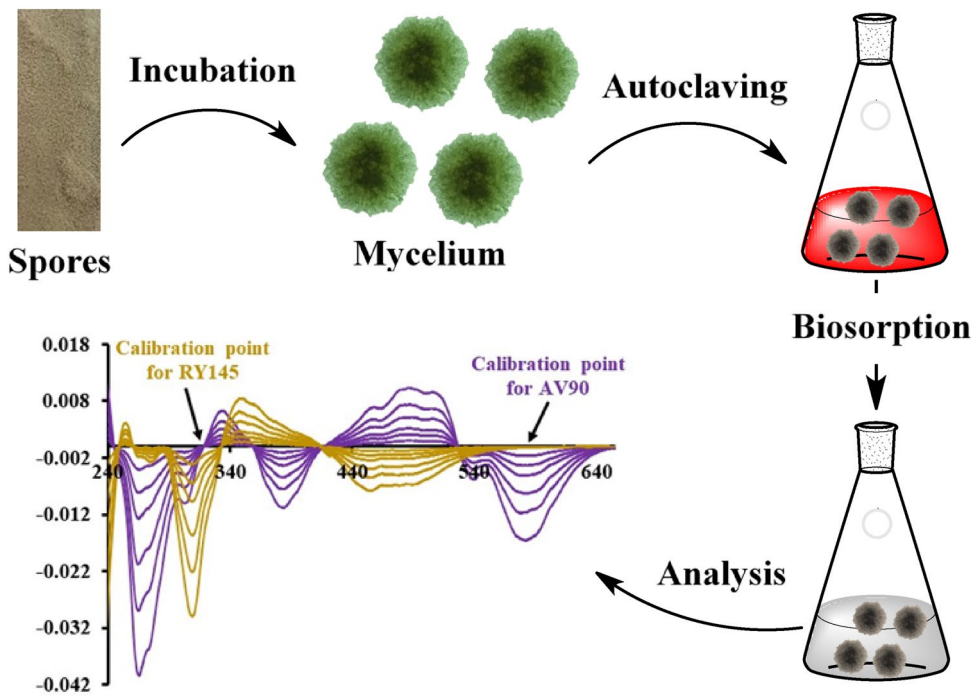

Biosorption process

Keywords *Cladosporium cladosporioides* · Biosorption · Acid Violet 90 · Reactive Yellow 145

Extended author information available on the last page of the article

Published online: 03 April 2024

Introduction

Treatment of textile dye wastes before discharge protects natural water resources. Several physical, chemical, and biological methods can be used for decolorization. The most widely used treatment processes are bacterial degradations, photocatalytic methods, and adsorption. Biosorption is also a type of adsorption where sorbents are loaded on biomass. Adsorption of organic matter on biomass can occur in many ways, such as electrostatic interaction, complexation, ion exchange, etc. Functional groups of biological molecules such as lipids and polysaccharides on the microorganism cell wall are involved in biosorption (Danouche et al. 2021). Both metallic (Heidarzadeh-Samani et al. 2023) and organic pollutants (Lima et al. 2023) can be removed from wastewater. Biomasses are also frequently used for decolorizing textile dye effluents such as cationic and anionic dyes removal by *Aspergillus parasiticus* (Bouras et al. 2021a), methylene blue by *Aspergillus carbonarius* and *Penicillium glabrum* (Bouras et al. 2021b), and Congo red and basic fuchsin by *Fusarium oxysporum* (Batana et al. 2022). C.I. Acid Violet 90 (AV 90) and C.I. Reactive Yellow 145 (RY145) are textile dyes with an aromatic azo structure. These dyes are classified as azo dyes and usually have water-soluble parts in addition to diazenyl groups (Benkhaya et al. 2020). The cleaved and uncleaved azo dyes can be carcinogenic to humans and animals. The aromatic amines are the cleaved products of azo dyes that can cause tumors and act as an allergen (Chung 2016). Some literature studies investigated the removal of acid violet and reactive yellow dyes via biosorption. *Zingiber officinale* and *Psidium guajava L.* powders were used in two works for the biosorption of AV90 (Hashem et al. 2023a, b). Both studies obtained the maximum removal at pH 2 using 0.2 g/L biosorbent. Caner et al. (2011) investigated biosorption of RY145 via dried *Penicillium restrictum.* The reported optimum removal pH is 1.0, the biomass dosage is 0.4 mg/L, and the agitation time is 75 min. Krishnasamy et al. (2022) used groundnut shell-based biochar to decolorize RY145. The equilibrium was obtained at pH 2 using 1.0 g/L biomass. Kifetew et al. (2023) prepared *teff* straw-activated carbon to remove RY145. The reported optimum removal parameters were pH 2, 0.3 g/L biomass dosage, and 120-min contact times. Zhang et al. (2003) used mycelium pellets from *Penicillium oxalicum* for the biosorption of RY145. The maximum percentages were obtained at pH 2. Benkaddour et al. (2018) treated watermelon seeds with hexane to remove RY145 at pH 3 using 1.0 g of biomass for 30 min. No biosorption studies on removing AV90 and RY145 individually or as a mixture by *Cladosporium cladosporioides* (CC) have been found in the literature. However, metal ion biosorption studies are available (Pethkar et al. 2001). Fungi spores are stored in a solid medium and can be reproduced over time. They are economical as there is no need for re-isolation or purchase. The biomass of fungus can be grown easily in large quantities when needed. They are also used on the industrial scale to purify textile dyes (Chicatto et al. 2018). Calculating individual organic substances concentration via absorption spectra becomes problematic when organic substances are found in mixtures. Derivative spectrophotometric methods are an easy way to solve this problem. The method is based on creating the calibration curve of a compound by using the zero crossing point of other substances in the derivative spectrum (Keskin et al. 2011).

In this study, *Cladosporium cladosporioides*, a fungus, was used as a biosorbent to remove the mixture of AV90 and RY145 simultaneously. Dead biomass was used in the experiments. The operational parameters affecting removals, such as pH, agitation time and speed, ambient temperature, dye concentrations, and biomass dosage, were investigated. A first-order derivative method was developed to analyze dye concentrations in the aqueous dye mixture. Fourier transform infrared spectroscopy (FTIR) was used to analyze the interaction between dead biomass and dyes to understand the sorption mechanism. Kinetic and isotherm studies were also performed.

Material and methods

The fungus *Cladosporium cladosporioides* MRC 70282 was purchased from The Scientific and Technological Research Council of Türkiye (TUBITAK) Marmara Research Center, Food Science and Technology Research Institute, Culture Collection Unit. The growth medium consisted of 20 g/L glucose, 5 g/L peptone, and 5 g/L yeast extract. An aliquot of spores was transferred to a previously autoclaved (121 °C for 20 min) growth medium (100 mL) and incubated at 28 °C and 160 rpm for five days (Yildirim et al. 2018). The obtained mycelium was autoclaved (121 °C, 20 min) to obtain dead biomass (Abdallah and Taha 2012). Then, it was filtered and washed with ethanol (Merck) and double distilled water. Finally, dead biomass was oven-dried at 50 °C, ground in a mortar, and stored in a desiccator.

All experiments were performed in the batch method, and all solutions were prepared using ultrapure water (Millipore). All glassware was purified using ethanol (Merck) for organic and diluted nitric acid (HNO_3) (Merck) for metallic interferences. AV90 and RY145 were obtained from a local textile factory. The effect of pH was investigated between 2 and 12, and the solution's pH was arranged

using 1.0 M hydrochloric acid (HCl) (Merck) and sodium hydroxide (NaOH) (Merck) by a pH meter. The point of zero charge (pH_{pzc}) was determined using 0.1 M potassium nitrate (KNO_3) and 0.1 g biomass. The final pH values were measured after 24 h. The graph was plotted between ΔpH (pH_f—pH_i) versus initial pH. The effect of contact time was examined between 15 and 120 min. The other affected parameter conditions are as follows: 50–200 rpm shaking speed, 20–50 °C ambient temperature, biomass dosage 0.05–0.50 g, and 25–150 mg/L dye concentrations. The absorbance of the dye solutions was measured at Shimadzu UV-2600 model ultraviolet–visible (UV–Vis) spectrophotometer at 200–800 nm wavelength ranges with 0.1 nm intervals. The solutions were centrifuged at 400 rpm before measurements. Characterization was done with Perkin Elmer (Spectrum Two) Fourier transform infrared (FTIR) spectrometer. Live and dead fungus pictures were taken under a microscope (Lecia DM500). The particle size distribution of biomass was measured using a NanoPlus zeta/nanoparticle analyzer. Biomass was dispersed in ultrapure water with an ultrasonic sonicator before measurement. The bulk density was calculated by dividing the weight of dead biomass by volume (Sadh et al. 2018). The biomass was filled into the cylinder with certain intervals to find its weight and volume. The difference between the full and empty cylinders gave the weight of biomass.

Results and discussion

The absorption and first-order derivative spectra of AV90 and RY145 are shown in Fig. 1. The absorption bands of the dyes overlap; therefore, simultaneous direct concentration determination in the mixture is impossible. The first-order derivative spectra have zero crossing points that can be used to prepare the calibration curve at 578.4 and 318.2 for AV90 and RY145. The calculated calibration equations, coefficients of determination (R^2), limit of detection (LOD), and limit of quantitation (LOQ) values of the method are shown in Table 1. The accuracy and precision of the method were calculated using 15 prepared synthetic mixtures. Mixture concentrations, recovery percentages (R%), and relative standard deviations (RSDs%) values are shown in Table 2. The calculated mean R% values are 100.2% for AV90 and 101.8% for RY145. The RSD% values are 1.5% and 1.1% for AV90 and RY145. The obtained values showed that the developed method was sufficient for the mixture analysis of these two dyes.

pH is the first examined parameter. It is the most critical for adsorption studies. Biosorption occurs with the functional groups onto the cell wall of dead biomass. These functional groups can ionize or vice versa, depending on the pH of the solution (Pace et al. 2009). Figure 2a shows the removal percentages of AV90 and RY145 at different pH solutions using 50 mg/L of each dye concentration and 0.1 g biomass. The biosorption degrees were decreased with the raised pH values. The removal percentages were higher at acidic pH values due to more significant electrostatic interactions

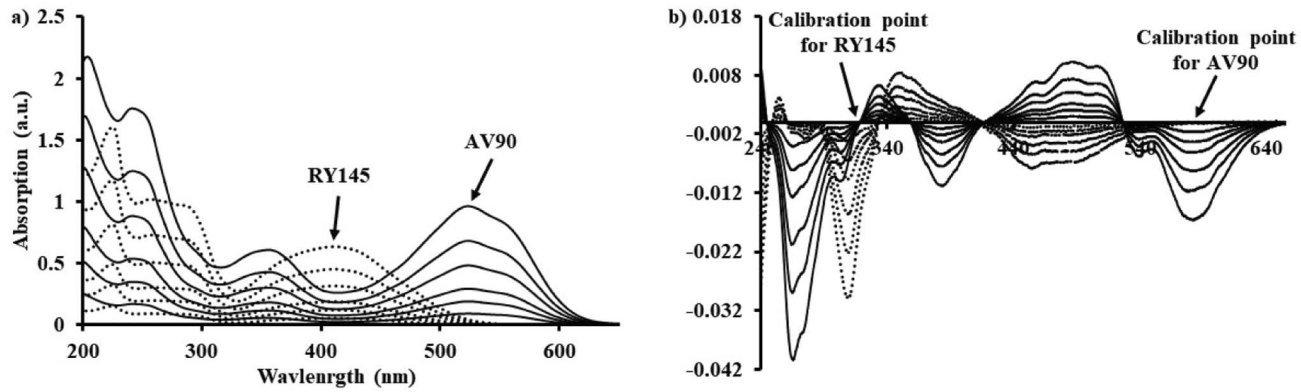

Fig. 1 Absorption (**a**) and first-order (**b**) spectra of AV90 and RY145

Table 1 Statistical parameters of the method

Dye	λ (nm)	Calibration equations	R^2	LOD (mg/L)	LOQ (mg/L)
RY145	318.2	$A = -0.00033C_{RY145} - 9.7 \times 10^{-6}$	0.9998	0.4546	1.5152
AV90	578.4	$A = -0.00033_{AV90} - 6.6 \times 10^{-5}$	0.9997	0.7423	2.4742

Table 2 Synthetic mixture concentrations, calculated R% and RSDs%

Mixture	Added (mg/L)		Found (mg/L)		Recovery (%)	
	AV90	RY145	AV90	RY145	AV90	RY145
1	5.0	5.0	4.9	5.1	97.9	101.7
2	10.0	10.0	10.0	10.2	99.9	102.0
3	15.0	15.0	15.6	14.8	104.0	98.7
4	25.0	25.0	24.8	25.6	99.1	102.2
5	35.0	35.0	35.0	35.8	99.9	102.2
6	50.0	50.0	51.3	51.1	102.6	102.3
7	5.0	50.0	4.9	50.6	97.9	101.2
8	10.0	35.0	10.0	35.8	99.9	102.2
9	15.0	25.0	15.1	25.0	100.6	100.2
10	25.0	15.0	24.8	15.3	99.1	102.1
11	35.0	10.0	35.0	10.2	99.9	102.0
12	50.0	5.0	50.8	5.1	101.6	101.7
13	35.0	5.0	35.0	5.1	99.9	101.7
14	25.0	50.0	25.3	51.1	101.1	102.3
15	10.0	35.0	10.0	36.3	99.9	103.7
				Mean	100.2	101.8
				SD	1.6	1.1
				RSD%	1.5	1.1

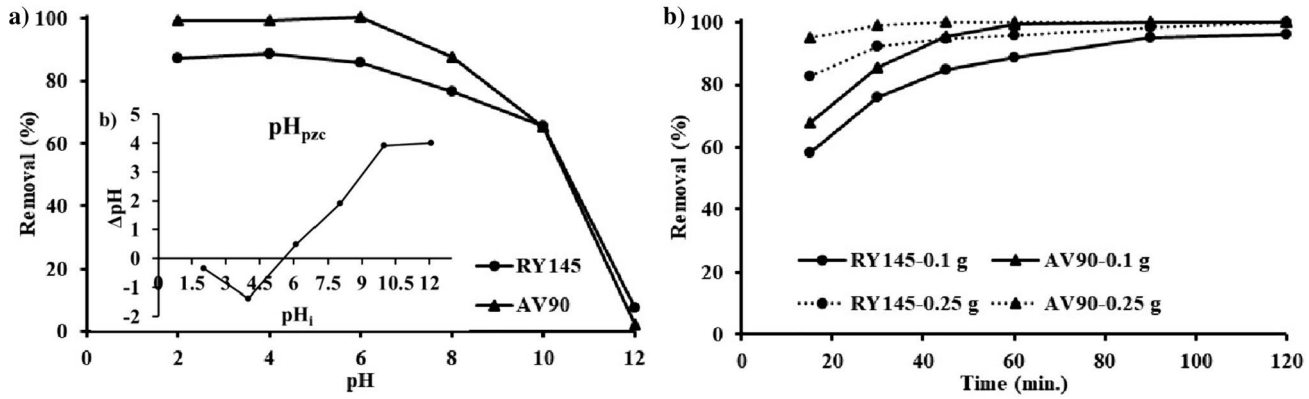

Fig. 2 The effect of pH (50 mg/L dyes, 60 min., 0.1 g biomass, 100 rpm agitation speed) (**a**), point of zero charge plot (**b**), and agitation time effect (pH 4, 50 mg/L dyes, 0.10 and 0.25 g biomass, 100 rpm agitation speed) (**c**) on removing AV90 and RY145

and formed hydrogen bonds at low pH values (Özacar and Şengil 2004). The groups on the biomass become positive via protonation and negative via hydrolysis at the acidic pH values. The determined pH_{pzc} value is 5.5 (Inset Fig. 2b). Below this pH, the amount of positively charged groups is greater than the number of negatively charged groups on the surface of the biomass. Conversely, if the pH is above 5.5, the amount of negatively charged groups will be more than that of positively charged groups (Srivastava and Hasan 2011). Both dyes have sulfonate groups ($-SO_3Na$) in their molecular structures (Table 3) that also efficiently ionize in acidic pH values and charge negative. Additionally, there is a protonatable amide group on the AV90. Thus, the structure of AV90 becomes positively and negatively charged at lower pH values. This zwitter ionic form provided more interaction between biomass and dye, resulting in higher removal percentages for AV90. The removal percentages were close in the acidic pH region for both dyes. The optimum pH was chosen as four since it is slightly higher. The negatively charged groups of the dyes were more attracted due to the higher amount of positively charged groups on the biomass surface at this pH. The equilibrium time of removal was investigated by performing biosorption at different periods using 0.10 and 0.25 g biomass (Fig. 2c). The removal was achieved 100% in a shorter time (60 min for RY145 and 30 min for AV90) when 0.25 g biomass was used. The effect

Table 3 Chemical structure and properties of AV90 and RY145 (National Center for Biotechnology Information 2024a and 2024b)

AV90	
Molecular formula	$C_{40}H_{30}CrN_8Na_2O_{10}S_2$
IUPAC name	Disodium;chromium;3-hydroxy-4-[(5-hydroxy-3-methyl-1-phenylpyrazol-4-yl)diazenyl] naphthalene-1-sulfonate;3-hydroxy-4-[(5-methyl-3-oxo-2-phenyl-1H-pyrazol-4-yl) diazenyl]naphthalene-1-sulfonate
CAS number	6408-29-3
Molecular weight	944.8 g/mol
Hazard statements	Eye Irrit. 2: causes serious eye irritation Aquatic Chronic 3: harmful to aquatic life with long-lasting effects
Molecular structure	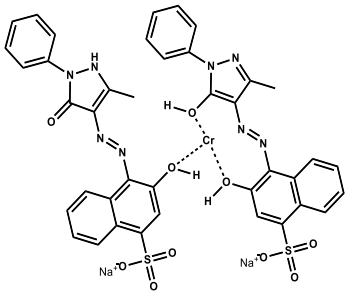
RY145	
Molecular formula	$C_{28}H_{20}ClN_9Na_4O_{16}S_5$
IUPAC name	Tetrasodium;7-[[2-(carbamoylamino)-4-[[4-chloro-6-[3-(2-sulfonatooxyethylsulfonyl) anilino]-1,3,5-triazin-2-yl]amino]phenyl]diazenyl]naphthalene-1,3,6-trisulfonate
CAS number	80157-00-2
Molecular weight	1026.3 g/mol
Hazard statements	Eye Irrit. 2: causes serious eye irritation Resp. Sens. 1: may cause allergy or asthma symptoms or breathing difficulties if inhaled
Molecular structure	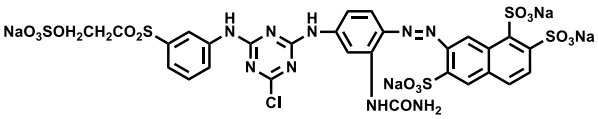

of time was seen more clearly when 0.10 g biomass was used. The maximum biosorption percentages reached 96% for RY145 and 100% for AV90 when using 0.10 g biomass in 90 and 120 min, respectively. The optimum time for the biosorption process was chosen as 60 min. The removal efficiency did not significantly change after equilibrium due to the complete coverage of active biomass sites. Shaking speed affects biosorption efficiency due to adjusted liquid film thickness around the biomass (Şahin et al. 2013). Lower shaking speeds cause higher film thickness, and the removal percentages were less (76% for RY145 and 89% for AV90 at 50 rpm). The film resistance was broken at fast speeds, and the removal rate increased to 92% for RY145 and 100% for AV90 at 150 rpm (Fig. 3a). The removal can decrease due to the reduced biomass-adsorbate interaction chance (or time) at higher shaking speeds. The temperature did not affect the biosorption process, and the removal percentages remained almost constant (Fig. 3b). The effect of biomass amount was examined in 50 and 100 mg/L (each of the dyes) mixture solutions (Fig. 3c). The mass impact can be more clearly discussed using higher concentrations of dyes. The efficiency reached 100% at 0.50 g and 0.10 g biomass for RY145 and AV90 when 50 mg/L dye was used in 60 min. The removal percentages increased from 55 to 93% for RY145 and 64% to 96% for AV90 when the biomass amount was increased from 0.05 to 0.50 g using 100 mg/L dye. The number of sites responsible for biosorption in the biomass increased, and more significant biomass-dye interactions occurred with the raised biomass amount. The effect of the initial dye concentration was evaluated with 25–150 mg/L of each dye concentration using 0.10 g and 0.25 g biomass (Fig. 3d). The removal percentages decreased with increased dye concentrations due to reduced not-interacted biomass sites. Nevertheless, 84% and 87% removal efficiencies were achieved for RY145 and AV90 when 0.25 g biomass and 150 mg/L dye were used. Considering the obtained results, it was concluded that AV90 should be biosorbed much more than RY145, but the removal percentages approached each

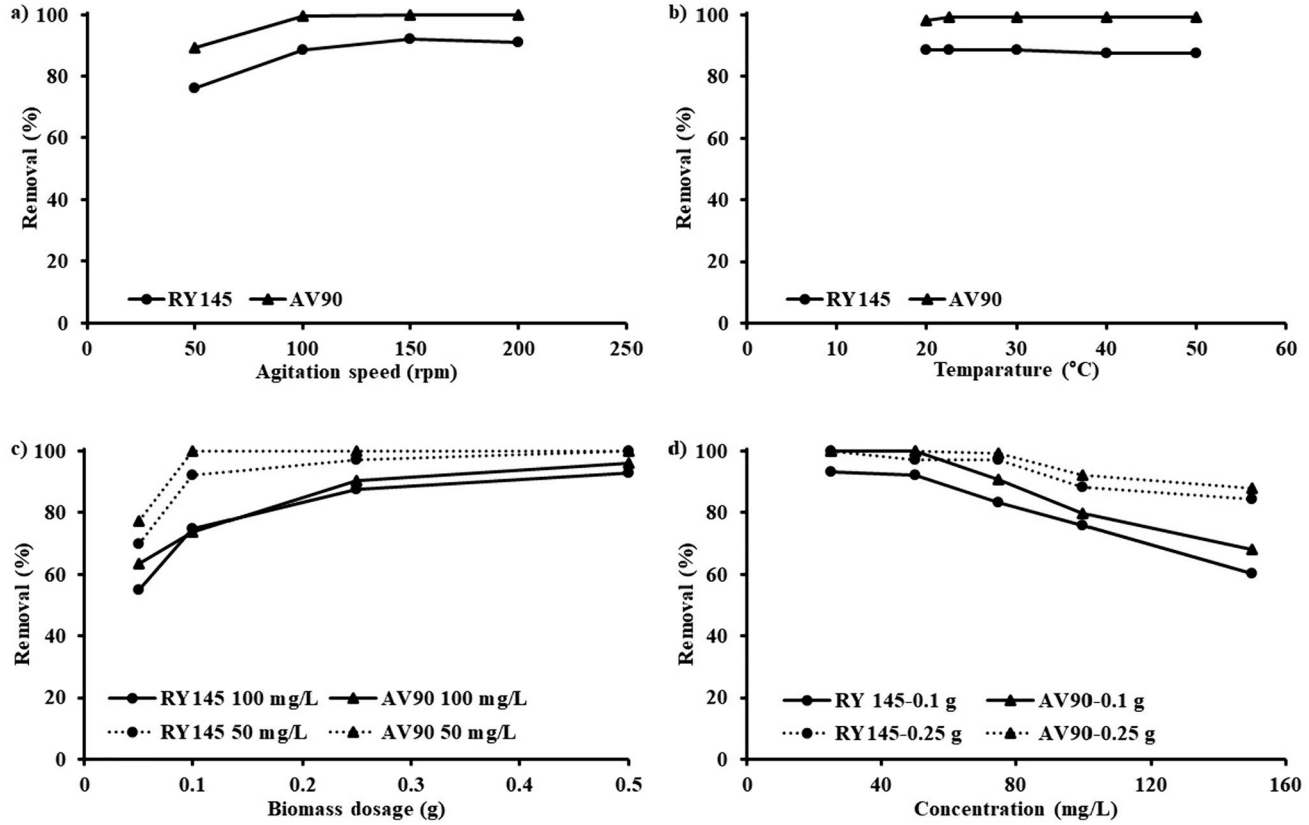

Fig. 3 The effect of agitation speed (pH 4, 50 mg/L dyes, 60 min., 0.1 g biomass) (**a**), ambient temperature (pH 4, 50 mg/L dyes, 60 min., 0.1 g biomass, 100 rpm agitation speed) (**b**), biomass dosage (pH 4, 50 and 100 mg/L dyes, 60 min., 150 rpm agitation speed) (**c**), each dye concentration (pH 4, 60 min., 0.10 and 0.25 g biomass, 150 rpm agitation speed) (**d**) on removing AV90 and RY 145

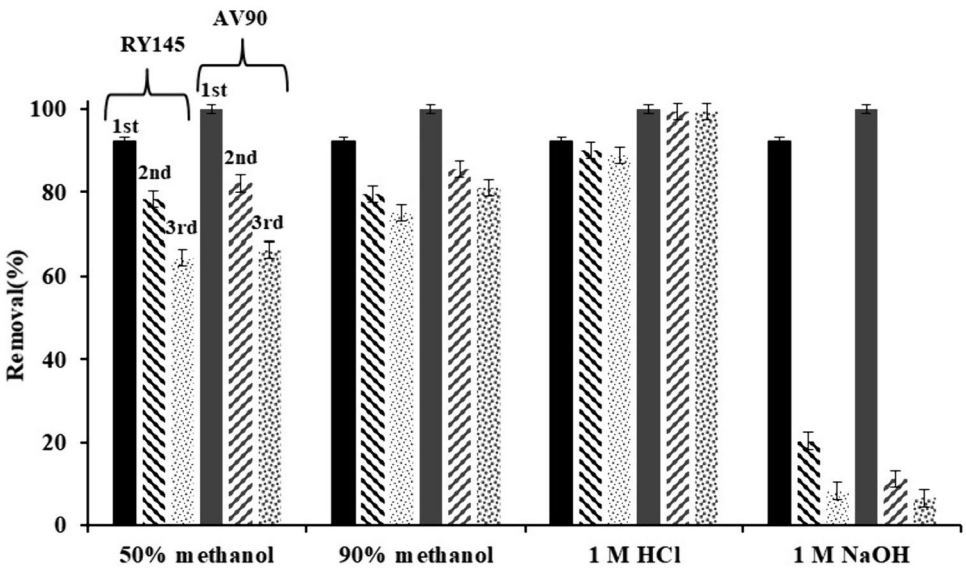

Fig. 4 The removal percentages of the adsorption–desorption cycles

other at high concentrations. This situation is compatible with the explanation that the interaction site of biomass is not enough at high dye concentrations. The reusability of the biomass was investigated by desorption experiments with 50% and 90% methanol, 1.0 M HCl, and 1.0 M NaOH solutions (Fig. 4). Acid and base solutions can remove mostly chemically bounded dye and regenerate biomass via H^+ or OH^- ion exchange. However, methanol can remove mostly

physically attached. The reuse experiments show that the worst desorption solution was NaOH; the best was HCl, and methanol had intermediate performance. The removal percentage decreased dramatically from 92 to 11% on the second use of NaOH-treated biomass, 7% on the third for RY145, 100% to 20% on the second use, and 8% on the third for AV90. The removal percentages decreased when methanol was used as the desorption solution. Although 90% methanol is better than 50% methanol, the mean removal values (~ 70% for RY145 and ~ 75 for AV90 in the third use) of reuse experiments are close for both dyes. Greater results were obtained with HCl-treated biomass. The removal percentages remained 89% for RY145 and 99% for AV90 in the third use of treated biomass. The results of methanol-treated biomass reuse experiments indicate the rate of physical interaction on the total removal is high. In addition, biosorbed dye amount by chemical bonding can also be considered high. The HCl solution was selected for desorption due to the capability of removing physically and chemically bounded dyes and regenerating the groups on the biomass. In addition, the treated biomass amount slightly decreased in each cycle (Table 4). The decreased amounts of biomass also had a role in reducing removal percentages.

Table 4 Amounts of reused biomass

Solution	1st (g)	2nd (g)	3rd (g)	Remained (g)
50% Methanol	0.1018	0.0912	0.0845	0.0816
90% Methanol	0.1013	0.0858	0.0833	0.0793
1.0 M HCl	0.1016	0.0908	0.0834	0.0766
1.0 M NaOH	0.1009	0.0800	0.0719	0.0628

The images of live and dead CC under the microscope are shown in Fig. 5. Dead biomass images were taken before and after biosorption. The biosorbed dyes on the dead biomass can be seen in the images. The particle size of dead biomass distribution is shown in Fig. 6. Particles uniformly have sizes ranging from 0.1 to 12.3 µm, and the calculated bulk density is 0.44 g/mL. FTIR analyses of dyes and dead biomass (before and after biosorption) were also performed (Fig. 7). In the FTIR spectrum of RY145, N–H, and O–H (due to the ionization of SO_3Na), stretching vibration bands overlapped at 3424 cm^{-1} (Singh et al. 2022). The 3091 cm^{-1} and 2925 cm^{-1} peaks are aromatic and aliphatic C–H stretching vibrations. RY145 contains a carbonyl diamide () group in the structure, so the carbonyl group stretching vibration peak (1753 cm^{-1}) appears higher than the usual wave number of the amide group. The peak at 1604 cm^{-1} appeared due to the C = N vibration. N = N and C = C vibration peaks overlapped at 1569 cm^{-1}. The peak at 1405 cm^{-1} belongs to the aromatic ring. The C–N vibration peaks appeared at 1174 cm^{-1}. The peaks at 1134 cm^{-1} and 1110 cm^{-1} occurred due to the SO_3 groups. The C–O and C–Cl vibration peaks appeared at 1037 cm^{-1} and 610 cm^{-1}. In the FTIR spectrum of AV90, the broad peak at ~ 3340 cm^{-1} belongs to overlapped bands of N–H and O–H stretching vibrations. Aromatic and aliphatic C–H stretching vibrations appeared at 3063 cm^{-1} and 2925 cm^{-1}. The 1661 cm^{-1} and 1597 cm^{-1} peaks belong to C = O and C = N vibrations. The overlapped bands of N = N and C = C groups appeared at 1541 cm^{-1}. The aromatic ring peak is at 1428 cm^{-1}. The peaks at 1184 cm^{-1} and 1157 cm^{-1} belong to the SO_3 group. The C–O vibration peak appeared at 1039 cm^{-1}.

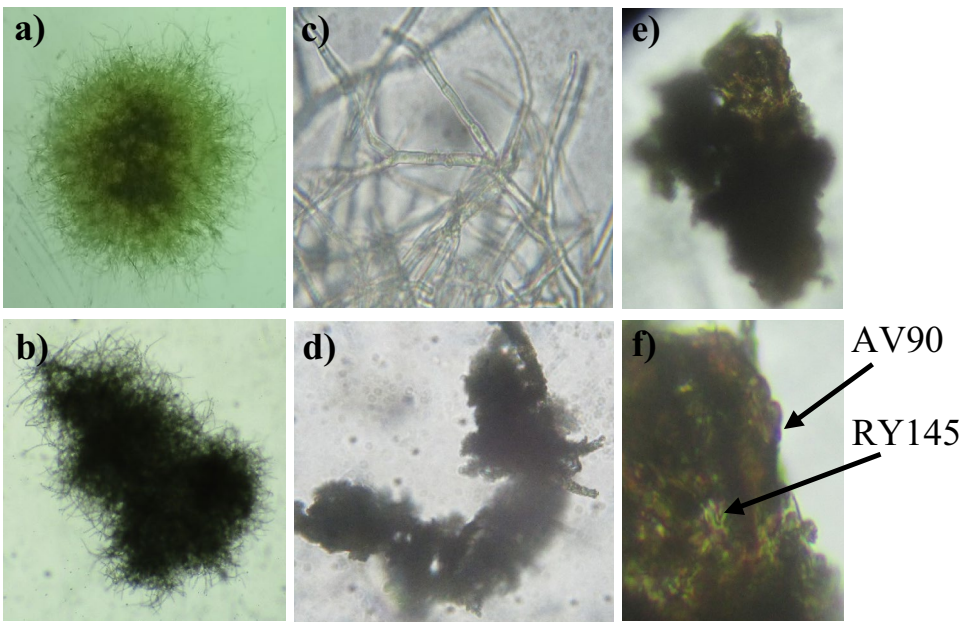

Fig. 5 Images of live (**a**, **b**, and **c**) and dead biomass before (**d**) and after (**e** and **f**) biosorption

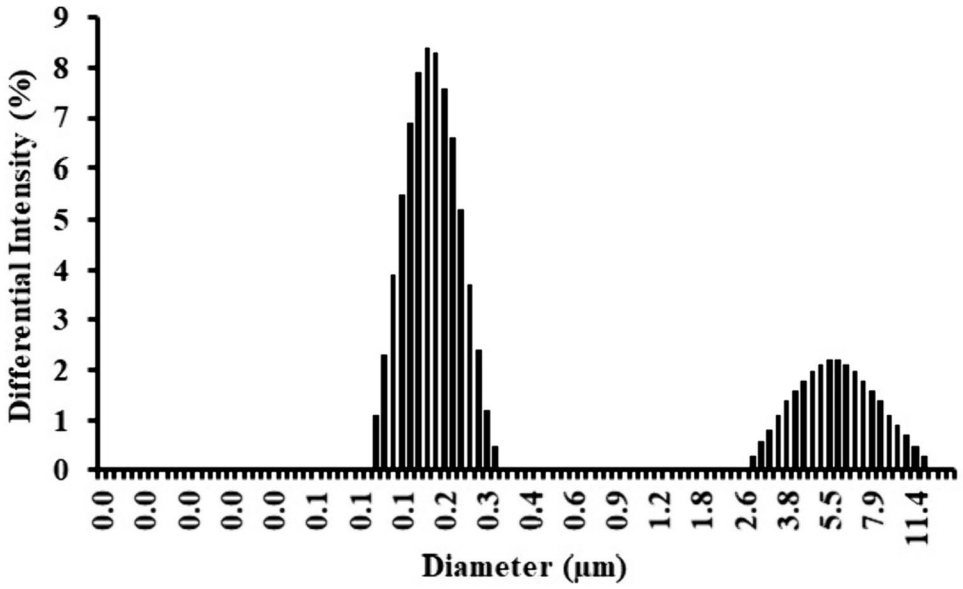

Fig. 6 Particle size distribution of biomass

The cell wall of the fungus generally contains proteins and carbohydrates with aromatic rings and different carbonyl groups (Gubbins and Anaissie 2009). The FTIR spectra of biomass and treated biomass are similar except for minor shifts. The 2924 cm^{-1}, 1538 cm^{-1}, and 1032 cm^{-1} peaks belong to aliphatic C–H, aromatic C = C and C–O group vibrations. The O–H and N–H vibration bands overlapped at 3276 cm^{-1} and 3280 cm^{-1} at the FTIR spectrum of biomass and treated biomass. The 1642 cm^{-1} and 1644 cm^{-1} peaks at biomass and treated biomass belong to the C = O group of amide. Most dye peaks overlapped and cannot seen beside fungus peaks. However, all peak intensities increase due to the added functional groups of dyes.

Kinetic parameters q_e (mg/g), k_1 (1/min), and k_2 (g/mg min) of biosorption were calculated using pseudo-first-order (1) and pseudo-second-order Eqs. (2) (Ho and McKay 1998).

$$\ln\left(q_e - q_t\right) = \ln q_e - kt \tag{1}$$

$$\frac{t}{q_t} = \frac{1}{k_2 q_e^2} + \frac{1}{q_e}\mathrm{t} \tag{2}$$

where q_e and q_t are the removed amount of dye at equilibrium and any time (t) and k_1 and k_2 are the rate constants. The calculated results are shown in Table 5. Both R^2 values of the kinetic models are high. The removal process better fits the pseudo-second-order, and the calculated q_e was higher than the pseudo-first-order kinetic model. It can be concluded that biosorption occurs by chemisorption (rate-limiting step) but also diffusion across the interface (Sahoo and Prelot 2020). It is consistent with the results of desorption experiments. Efficient desorption could not be achieved using solvent (methanol) alone. Acid regeneration was required to eliminate chemisorption. The linear model of Langmuir, Freundlich, Sips, Dubinin–Radushkevich, and Temkin's adsorption isotherm was also investigated (Table 6). The constants were calculated by Eqs. (3), (4), (5), (6), and (7) (Popoola 2019).

$$\frac{C_e}{q_e} = \frac{1}{Q_0 b} + \frac{C_e}{Q_0} \tag{3}$$

$$\log q_e = \log K_f + \frac{1}{n}\log C_e \tag{4}$$

$$\ln\left(\frac{q_e}{q_m - q_e}\right) = \frac{1}{n}\ln \mathrm{C_e} + \ln\left(b_s\right)^{\frac{1}{n}} \tag{5}$$

$$\ln q_e = \ln q_m - B_D \varepsilon^2 \tag{6}$$

$$q_e = b_T \ln A_T + b_T \ln C_e \tag{7}$$

where the Q_0 (mg/g) is the adsorption capacity of biomass, C_e is the residual equilibrium concentration of dye, b (L/mg) is the energy of adsorption, K_f (mg/g) is the biosorption capacity, n is the biosorption intensity, q_m (mg/g) is the maximum adsorption capacity, b_s is the Sips isotherm constant, B_D (mol^2/kJ^2) Dubinin–Radushkevich isotherm constant, ε is the Polanyi potential, A_T (L/mg) is the equilibrium binding constant, b_T (J/mol) is the Temkin constant. The R^2 values of Langmuir isotherm for both dyes are higher than for other isotherms. The biosorption better fits the Langmuir

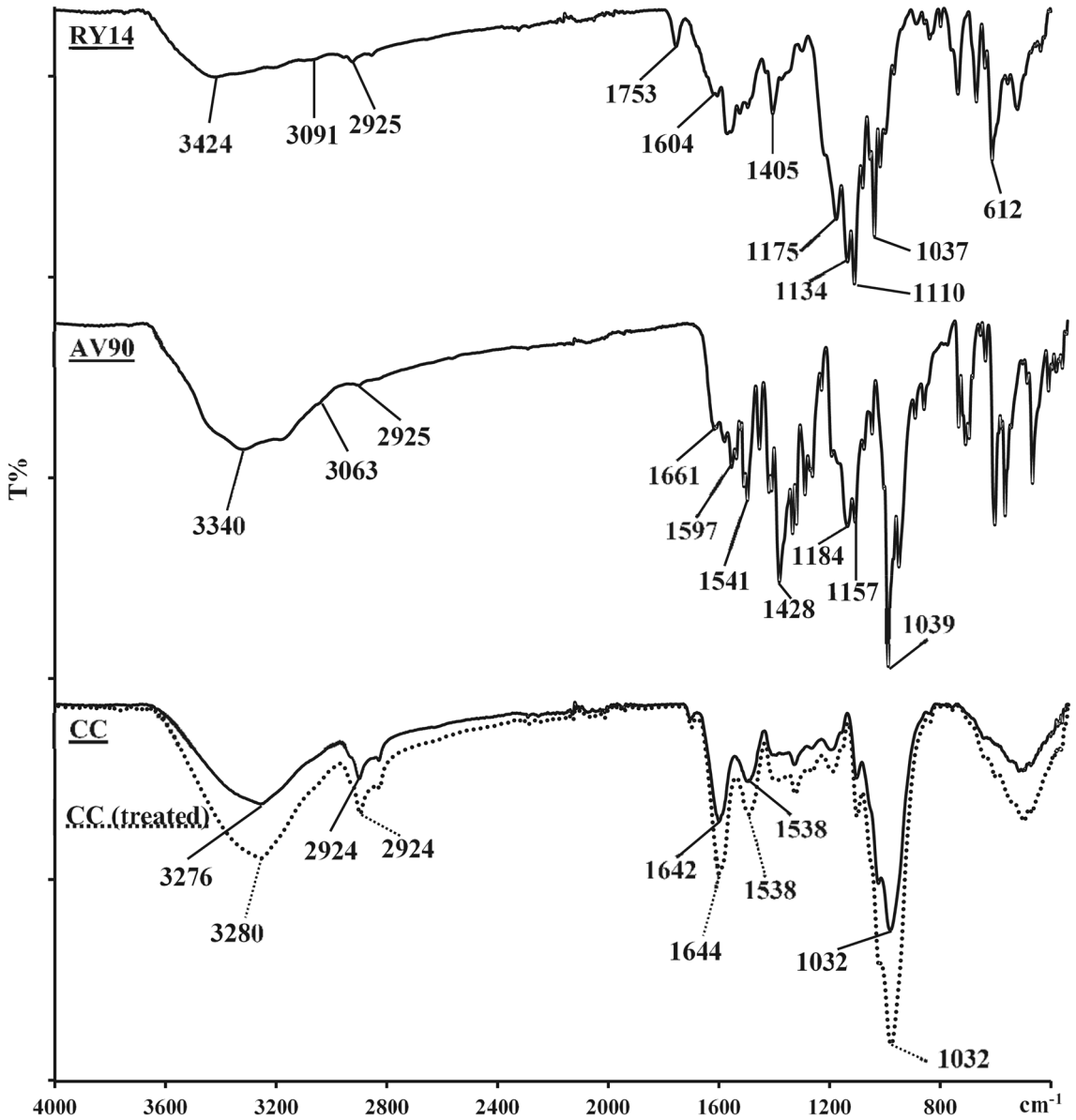

Fig. 7 FTIR spectra of RY145, AV90, biomass, and treated biomass

Table 5 Kinetic parameters

Pseudo-first-order			
Dye	q_e (mg/g)	k_1 (1/min)	R^2
RY145	7.0682	0.0172	0.9977
AV90	7.3181	0.0177	0.9979
Pseudo-second-order			
Dye	q_e (mg/g)	k_2 (g/mg min)	R^2
RY145	24.2017	0.0058	0.9995
AV90	18.7863	0.0051	0.9994

Table 6 Calculated constants of isotherms

Isotherms	Parameters	RY145	AV90
Langmuir	Q_0 (mg/g)	24.9610	27.0738
	b (L/mg)	0.1746	0.6540
	R^2	0.9972	0.9902
Freundlich	K_f (mg/g)	5.9518	16.2050
	n	2.7714	9.1131
	R^2	0.9034	0.8298
Sips	b_s (L/g)	0.2090	2.7182
	n	0.9020	2.8409
	R^2	0.9835	0.6927
Dubinin–Radushkevich	B_D (mol^2/kJ^2)	0.9522	0.0047
	q_m (mg/g)	18.9807	21.9295
	R^2	0.9307	0.8418
Temkin	b_T (kJ/mol)	4.7487	1.5615
	A_T (L/mg)	2.5080	9.5003
	R^2	0.9793	0.8591

isotherm, and the adsorption capacity (Q_0) is higher than the calculated other isotherm value. It can be concluded that the removal occurs in a monolayer, so the active sites of the biomass can interact with only one molecule of dye (Kalam et al. 2021). It is agreed with the experimental results that the removal percentage increased with the raised biosorbent amount. Adsorption thermodynamics parameters were not investigated because temperature did not affect biosorption.

Conclusions

An efficient biosorption method was developed to remove a mixture of AV90 and RY145 textile dyes. The dead form of a *Cladosporium* genus was used. The first-order derivative method was used to analyze the dye in the mixture solution. The removal efficiency was achieved at 100% using 0.25 g biomass and 50 mg/L of each dye concentration in pH 4, 60 min agitation time, and 150 rpm shaking speed. The calculated adsorption capacities of biomass are ~ 24 mg/g for RY145 and ~ 27 mg/g for AV90. The biosorption mechanism is well fitted with pseudo-second-order kinetic and Langmuir isotherm. It is concluded that chemisorption was the rate-limiting step, but physical sorption was also high, and monolayer adsorption was carried out. The FTIR analyses also show there are suitable functional groups on dyes and biomass for biosorption. The biomass can be used efficiently to remove dye mixtures repeatedly after regeneration. The removal efficiency is still high (89% for RY145 and 99% for AV90) after being treated with HCl, and it can be concluded that the biomasses from CC can be reused on an industrial scale for textile wastewater treatment. Previous studies that used fungus as a biosorbent focused on single-dye removal. However, more than one organic material may be in natural waters or wastewater, and that causes difficulties in analysis. Therefore, different methods must be derived to analyze actual samples. The developed first-order derivative method can be performed in combined water treatment, and future studies should be focused on proving the usability of the developed method on an industrial scale.

Acknowledgments The authors would like to thank Assoc. Prof. Hatice Tunca (Department of Biology, Faculty of Sciences, Sakarya University) for her help with microscope images, and Dr. Burak Ünlü (Biomedical, Magnetic and Semiconductor Materials Application and Research Center, Sakarya University) for his help with particle size analysis.

Author contribution All authors contributed to the study's conception and design. SYK and MCT performed biomass preparation and investigation of parameters. FTIR analysis, development and application of the derivative method, calculation of kinetic and isotherm parameters, and manuscript writing were carried out by Can Serkan Keskin. All authors read and approved the final manuscript.

Funding Open access funding provided by the Scientific and Technological Research Council of Türkiye (TÜBİTAK). This work was supported by Scientific Research Projects Coordinator of Sakarya University under grant number 2024-26-62-18.

Data availability Not applicable.

Code availability Not applicable.

Declarations

Conflict of interest The authors declare no competing interests.

Ethics approval Not applicable.

Consent to participate Not applicable.

Consent for publication Not applicable.

References

Abdallah R, Taha S (2012) Biosorption of methylene blue from aqueous solution by nonviable Aspergillus fumigatus. Chem Eng J 195–196:69–76. https://doi.org/10.1016/j.cej.2012.04.066

Batana FZ, Bouras HD, Aouissi H (2022) Biosorption of congo red and basic fuchsin using micro fungi *Fusarium oxysporum* F. Sp. *Pisi* as a biosorbent: modeling optimization and kinetics study. Egypt J Chem 65:225–235. https://doi.org/10.21608/EJCHEM.2022.113994.5188

Benkaddour S, Slimani R, Hiyane H et al (2018) Removal of reactive yellow 145 by adsorption onto treated watermelon seeds: kinetic and isotherm studies. Sustain Chem Pharm 10:16–21. https://doi.org/10.1016/j.scp.2018.08.003

Benkhaya S, M'rabet S, El Harfi A (2020) Classifications, properties, recent synthesis and applications of azo dyes. Heliyon 6:e03271. https://doi.org/10.1016/j.heliyon.2020.e03271

Bouras HD, RédaYeddou A, Bouras N et al (2021a) Biosorption of cationic and anionic dyes using the biomass of *Aspergillus parasiticus* CBS 100926^{T}. Water Sci Technol 83:622–630. https://doi.org/10.2166/wst.2021.005

Bouras HD, Isik Z, Arikan EB et al (2021b) Biosorption characteristics of methylene blue dye by two fungal biomasses. Int J Environ Stud 78:365–368. https://doi.org/10.1080/00207233.2020.1745573

Caner N, Kiran I, Ilhan S et al (2011) Biosorption of reactive yellow 145 dye by dried Penicillum restrictum: Isotherm, kinetic, and thermodynamic studies. Sep Sci Technol 46:2283–2290. https://doi.org/10.1080/01496395.2011.585211

Chicatto JA, Gonçalves MJ, Altmajer-Vaz D, Tavares LBB (2018) Treatment of the textile wastewater through fungi: a sustainable alternative. Sustentabilidade Em Debate - Brasília 9:198–213. https://doi.org/10.18472/SustDeb.v9n1.2018.26460

Chung KT (2016) Azo dyes and human health: A review. J Environ Sci Health C Environ Carcinog Ecotoxicol Rev34:233–261. https://doi.org/10.1080/10590501.2016.1236602

Danouche M, El Arroussi H, Bahafid W, El Ghachtouli N (2021) An overview of the biosorption mechanism for the bioremediation of synthetic dyes using yeast cells. Environ Technol Rev 10:58–76. https://doi.org/10.1080/21622515.2020.1869839

Gubbins PO, Anaissie EJ (2009) Antifungal therapy. In clinical mycology. Elsevier Inc., pp 161–195. https://doi.org/10.1016/B978-1-4160-5680-5.X0001-1.

Hashem A, Aniagor CO, Farag S, Aly AA (2023a) Adsorption of acid violet 90 dye onto activated carbon and guava seed powder adsorbents. Biomass Convers Biorefinery 19:1–5. https://doi.org/10.1007/s13399-023-04758-w

Hashem A, Dubey S, Sharma YC et al (2023b) Zingiber officinale powder as a biosorbent for adsorption of acid violet 90 from aqueous solutions. Biomass Convers Biorefinery 20:1–6. https://doi.org/10.1007/s13399-023-04488-z

Heidarzadeh-Samani M, Behzad T, Mehrabani-Zeinabad A, Baghbadorani NB (2023) Removal of chromium ions by a bionanocomposite hydrogel based on starch-g-poly(acrylic acid) reinforced by cellulose nanofibers through a fix-bed adsorption column. Clean Technol Environ Policy 24:1–2. https://doi.org/10.1007/s10098-023-02623-y

Ho YS, McKay G (1998) The kinetics of sorption of basic dyes from aqueous solution by sphagnum moss peat. Can J Chem Eng 76:822–827. https://doi.org/10.1002/cjce.5450760419

Kalam S, Abu-Khamsin SA, Kamal MS, Patil S (2021) Surfactant adsorption isotherms: a review. ACS Omega 6:32342–32348. https://doi.org/10.1021/acsomega.1c04661

Keskin CS, Özdemir A, Şengil IA (2011) Simultaneous decolorization of binary mixture of reactive yellow and acid violet from wastewaters by electrocoagulation. Water Sci Technol 63:1644–1650. https://doi.org/10.2166/wst.2011.306

Kifetew M, Alemayehu E, Fito J et al (2023) Adsorptive removal of reactive yellow 145 dye from textile industry effluent using Teff Straw Activated Carbon: optimization using central composite design. Water (switzerland) 15:1281. https://doi.org/10.3390/w15071281

Krishnasamy S, Saiatchyuth BA, Ravindiran G et al (2022) Effective removal of reactive yellow 145 (RY145) using Biochar Derived from Groundnut Shell. Adv Mater Sci Eng 2022:8715669. https://doi.org/10.1155/2022/8715669

Lima FA, de Júnior AMF, Sarrouh B, Lofrano RCZ (2023) Application of sugarcane bagasse and peanut shell in natura as bioadsorbents for vinasse treatment. Clean Technol Environ Policy. https://doi.org/10.1007/s10098-023-02650-9

National Center for Biotechnology Information (2024a) PubChem Compound Summary for CID 136496748, Acid Violet 90. Retrieved February 1, 2024 from https://pubchem.ncbi.nlm.nih.gov/compound/Acid-Violet-90

National Center for Biotechnology Information (2024b) PubChem Compound Summary for CID 157317, C.I. Reactive Yellow 145. Retrieved February 1, 2024 from https://pubchem.ncbi.nlm.nih.gov/compound/C.I.-Reactive-Yellow-145

Özacar M, Şengil IA (2004) Equilibrium data and process design for adsorption of disperse dyes onto Alunite. Environ Geol 45:762–768. https://doi.org/10.1007/s00254-003-0936-5

Pace CN, Grimsley GR, Scholtz JM (2009) Protein ionizable groups: pK values and their contribution to protein stability and solubility. J Biol Chem 284:13285–13289. https://doi.org/10.1074/jbc.R800080200

Pethkar AV, Kulkarni SK, Paknikar KM (2001) Comparative studies on metal biosorption by two strains of *Cladosporium cladosporioides*. Bioresour Technol 80:211–215. https://doi.org/10.1016/s0960-8524(01)00080-3

Popoola LT (2019) Characterization and adsorptive behaviour of snail shell-rice husk (SS-RH) calcined particles (CPs) towards cationic dye. Heliyon 5:e01153. https://doi.org/10.1016/j.heliyon.2019.e01153

Sadh PK, Chawla P, Bhandari L, Duhan JS (2018) Bio-enrichment of functional properties of peanut oil cakes by solid state fermentation using *Aspergillus oryzae*. J Food Meas Charact 12:622–633. https://doi.org/10.1007/s11694-017-9675-2

Şahin İ, Keskin SY, Keskin CS (2013) Biosorption of cadmium, manganese, nickel, lead, and zinc ions by *Aspergillus tamarii*. Desalination Water Treat 51:4524–4529

Sahoo TR, Prelot B (2020) Adsorption processes for the removal of contaminants from wastewater: the perspective role of nanomaterials and nanotechnology. In micro and nano technologies. Elsevier Inc., pp. 161–222. https://doi.org/10.1016/B978-0-12-818489-9.00007-4

Singh AL, Chaudhary S, Kumar S, Kumar A, Singh A, Yadav A (2022) Biodegradation of reactive yellow-145 azo dye using bacterial consortium: a deterministic analysis based on degradable Metabolite, phytotoxicity and genotoxicity study. Chemosphere 300:134504

Srivastava P, Hasan SH (2011) Biomass of mucor heimalis for the bıosorption of cadmıum from aqueous solutions: equilibrium and kinetic studies. BioResources 64:3656–3675. https://doi.org/10.15376/biores.6.4.3656-3675

Yildirim K, Kuru A, Yılmaz RF (2018) Microbial transformation of some steroids by *Cladosporium cladosporioides* MRC 70282. J Chem Res 42:408–411. https://doi.org/10.3184/174751918X15337219180719

Zhang SJ, Yang M, Yang QX et al (2003) Biosorption of reactive dyes by the mycelium pellets of a new isolate of Penicillium oxalicum. Biotechnol Lett 25:1479–1482. https://doi.org/10.1023/A:1025036407588

Authors and Affiliations

Can Serkan Keskin[1] · Semra Yılmazer Keskin[1] · Mehmet Can Topcu[2]

✉ Can Serkan Keskin
ckeskin@sakarya.edu.tr

[1] Department of Chemistry, Faculty of Science, Sakarya University, 54050 Serdivan, Sakarya, Türkiye

[2] Institute of Natural Sciences, Sakarya University, 54050 Serdivan, Sakarya, Türkiye